Cell Motility and the Cytoskeleton 41:202–213 (1998)

Xenopus Interphase and Mitotic Microtubule-Associated Proteins Differentially Suppress Microtubule Dynamics In Vitro

Søren S.L. Andersen*

European Molecular Biology Laboratory, Cell Biology Program, Heidelberg, Germany

Based on observations of microtubule dynamics in *Xenopus* extracts and in vivo, it has been assumed that the pool of interphase microtubule-associated proteins (MAPs) are more potent microtubule stabilizers than their mitotic counterparts. The aim of this study was to test that assumption, and two questions were addressed here. First, are there differences in the composition of interphase and mitotic MAPs? Second, do interphase MAPs more potently promote microtubule assembly than mitotic MAPs? Biochemical purification from *Xenopus* egg extracts shows that the composition of interphase and mitotic MAPs is similar. XMAP215, XMAP230, and XMAP310, which are the three characterized *Xenopus* MAPs, show decreased microtubule binding in mitotic extracts, and mitotic MAPs are slightly more phosphorylated than interphase MAPs. Bulk polymerization and time-lapse video microscopy show that microtubules polymerized two times faster in the presence of total interphase MAPs compared with total mitotic MAPs. Interphase but not mitotic MAPs strongly promoted microtubule nucleation in solution. Video microscopy showed that microtubules never underwent catastrophes in the presence of either MAP fraction. It is proposed that the increase in microtubule dynamics at the onset of mitosis results from phosphorylation dependent decreased microtubule stabilization by MAPs, allowing destabilizing factors to increase the catastrophe frequency and dismantle the interphase microtubule network. Cell Motil. Cytoskeleton 41:202–213, 1998.

Key words: microtubule dynamics reconstitution; phosphorylation; cell cycle; regulation; Stathmin/Op18; XKCM1

INTRODUCTION

Formation of the mitotic (M) spindle requires depolymerization of the interphase (I) microtubule (MT) network, followed by selective MT growth around chromosomes. This reorganization involves a change in MT turnover/dynamics at the onset of mitosis (M) [Andersen, 1999a; Hyman and Karsenti, 1996; Inoué and Salmon, 1995; Waters and Salmon, 1997]. The turnover/dynamics of MTs relevant for this paper is best described by the *dynamic instability* model [Kirschner and Mitchison, 1986; Mitchison and Kirschner, 1984b]. In this model, a MT polymerizes with a certain *growth rate* (v_g), and depolymerizes with a certain *shrinkage rate* (v_s). The transition from growth to shrinkage is called a *catastrophe* [McIntosh, 1984] and occurs with a certain frequency

Abbreviations: f_{cat}, catastrophe frequency; f_{res}, rescue frequency; I, interphase; M, mito-tic/sis; MAP, microtubule-associated protein; MT, microtubule; v_g, growth rate; v_s, shrinkage rate.

*Correspondence to: Søren S.L. Andersen (current address): University of California at San Diego, Department of Biology, 9500 Gilman Drive, La Jolla, CA 92093-0357; E-mail: sandersen@ucsd.edu

Received 4 March 1998; accepted 17 July 1998.

(f_{cat}). The opposite event, from shrinkage to growth, is called a *rescue* and occurs with a certain frequency (f_{res}) [Walker et al., 1988]. MTs may also turnover by so-called *treadmilling,* where tubulin subunits continuously added to one end of a MT are subsequently lost by continuous depolymerization at the other end [Hotani and Hori, 1988; Vorobjev et al., 1997; Waterman-Storer and Salmon, 1997].

A required step towards elucidation of the mechanism of spindle assembly is to understand the process of MT dynamics regulation at the I-to-M transition. It is clear that the dynamics of pure MTs in vitro [i.e., Chrétien et al., 1995] are different from the dynamics observed in vivo in both I an M [Belmont et al., 1990; Cassimeris et al., 1988; Sammak and Borisy, 1988; Schulze and Kirschner, 1988; Shelden and Wadsworth, 1993; Tanaka and Kirschner, 1991; Tournebize et al., 1997; Verde et al., 1992; summarized by Andersen, 1995]. These differences cannot be explained by a difference in the free tubulin concentration between the in vivo and the in vitro conditions because the parameters of MT dynamics were determined in vitro at a tubulin concentration of about 10–20 μM, which is close to the range of tubulin concentrations measured in vivo [Cassimeris et al., 1988; Hiller and Weber, 1978; Houliston and Elinson, 1992; Zhai et al., 1996]. Moreover, although pure MTs to some extend are inherently dynamic [Billger et al., 1996; Chrétien et al., 1995], there must be additional factors regulating MT dynamics in vivo.

A roughly 10-fold increase in f_{cat} represents the most dramatic change in MT dynamics between I and M, and can account for the changes in dynamics observed between I and M [Gliksman et al., 1993; Verde et al., 1992]. This change in f_{cat} is regulated by cdc2 kinase [Belmont et al., 1990; Ookata et al., 1997; Tournebize et al., 1997; Verde et al., 1992; Verde et al., 1990], and probably other kinases [Drewes et al., 1997; Gotoh et al., 1991] and phosphatases [Andreassen et al., 1998; Gliksman et al., 1992; Howell et al., 1997; Tournebize et al., 1997]. While the molecular targets of these kinases and phosphatases are largely unknown, microtuble-associated proteins (MAPs) are good candidates since they promote MT assembly less efficiently in their more phosphorylated, mitotic, form than in their less phosphorylated, interphase, form [Andersen et al., 1994; Burns et al., 1984; Drechsel et al., 1992; Drewes et al., 1997; Illenberger et al., 1996; Itoh et al., 1997; Masson and Kreis, 1995; Olmsted et al., 1989; Ookata et al., 1995, 1997; Scott et al., 1993; Shiina et al., 1992].

MAPs were discovered as contaminants when tubulin was first purified from neuronal tissues [i.e., Cleveland et al., 1977; Herzog and Weber, 1978; Weisenberg, 1972], and at present seven main groups of proteins are known to interact with and affect MT polymerization: structural MAPs, motors, MT-linked enzymes, and MT modifying enzymes, proteins copurifying with MTs, MT severing factors and soluble proteins [reviewed by Hirokawa, 1994; Hyams and Lloyd, 1994; Mandelkow and Mandelkow, 1995; Olmsted, 1986; Wiche et al., 1991]. The proteins of primary interest to this work are proteins that copurify with MTs. Most of these proteins are structural MAPs/bona fide MAPs, which means that they in pure form can bind back to MTs.

How do MAPs regulate MT dynamics? Several studies report on the effect of single as well as populations of neuronal MAPs on MT dynamics in vitro and in vivo [i.e., Bré and Karsenti, 1990; Dhamodharan and Wadsworth, 1995; Drechsel et al., 1992; Itoh and Hotani, 1994; Pryer et al., 1992]. The summary of these in vitro experiments is that neuronal MAPs suppress MT dynamics and promote spontaneous assembly by efficiently suppressing f_{cat} and increasing v_g.

Our knowledge about how somatic MAPs affect MT turnover/dynamics in vitro have to date focused on the modulation by individual molecules [Andersen et al., 1994; Andersen and Karsenti, 1997; Hamill et al., 1998; Ookata et al., 1995; Vasquez et al., 1994]. However, in vivo and in *Xenopus* egg extracts numerous MAPs, motors, and other molecules interact with and influence MT polymerization dynamics simultaneously, and are competing with each other for interaction with the MT lattice [Belmont and Mitchison, 1996; Bulinski et al., 1997; López and Sheetz, 1995; Mandelkow and Mandelkow, 1995; Shiina et al., 1992; Vale, 1991; Walczak et al., 1996, 1998]. The sum of these interactions must determine the dynamic state of MTs during the cell cycle in vivo. However, no studies have looked at how the population of somatic structural MAPs that bind to MTs in extracts affect MT dynamics in vitro.

As a first step toward reconstitution of in vivo MT dynamics in vitro, this study compared the in vitro activity differences between *Xenopus* I and M MAPs with MT dynamics observed in *Xenopus* egg extracts and in vivo. The differential effects of I and M MAPs on MT polymerization dynamics reported here partially reconstitutes the changes in MT dynamics from I to M observed in *Xenopus* egg extracts and in vivo [Belmont et al., 1990; Tournebize et al., 1997; Verde et al., 1992; Zhai et al., 1996]. The most important difference between this in vitro study and the *Xenopus* extract data is the complete absence of catastrophes in the presence of both I and M MAPs. It is proposed that in the extract and in vivo, the increase in MT dynamics at the onset of mitosis results from phosphorylation dependent decreased MT stabilization by MAPs, allowing destabilizing factors, such as Stathmin/Op18, Kar3, and XKCM1, to increase the MT

catastrophe frequency [Andersen et al., 1997; Belmont and Mitchison, 1996; Curmi et al., 1997; Huyett et al., 1998; Walczak et al., 1996].

MATERIALS AND METHODS

Preparation of Extracts

CSF-arrested *Xenopus* egg extracts and buffers were prepared according to Murray [1991]. *Xenopus* egg extracts are considered a quasi in vivo situation because all the necessary components for MT dynamics, formation of functional mitotic spindles and interphase nuclei are present in the extracts [Belmont et al., 1990; Murray, 1991; Shamu and Murray, 1992; Tournebize et al., 1997]. In order to have extracts as identical as possible, I extracts were derived from M extracts by addition of 0.5 mM $CaCl_2$ and 200 µg/ml cycloheximide for 40 min at 20°C [Shamu and Murray, 1992]. Alternatively, cyclinBΔ90 [Glotzer et al., 1991] plus 200 µg/ml cycloheximide was added to activate (for 45 min at 20°C) I extracts to enter M. Before MAP preparations (see below), extracts were centrifuged at 100,000*g*, 30 min, 2°C. This supernatant had histone H1 kinase activities [Félix et al., 1994] of 12–20 and 2–4 pmoles/µl/min for M and I extracts, respectively. Alternatively, MAPs were prepared (see below) from extracts diluted 1:1 with cold CSF-XB (100 mM KCl, 50 mM sucrose, 2 mM $MgCl_2$, 5 mM EGTA, 0.1 mM $CaCl_2$, 10 mM Hepes, pH = 7.7) and centrifuged at 100,000*g* for 30 min, 2°C.

Purification of MAPs

MAPs were prepared as described by Andersen et al. [1994]. However, MAPs were bound to MTs at room temperature, not 37°C, with one additional modification: 1 µM micro-cystin LR (Gibco BRL #13130-026 stock: 1 mM in DMSO) was added to the sucrose cushions to inactivate phosphatases. Micro-cystin [MacKintosh and MacKintosh, 1994] does not inhibit kinases, and is a very potent, irreversible and specific inhibitor of PP1 and PP2A phosphatases which are abundant in *Xenopus* egg extract [Tournebize et al., 1997]. Note that I and M MAPs were prepared from the same primary extract, which is essential, as there are significant variations between extracts. The MAPs were eluted from the MT pellet with 400 mM NaCl in BRB80, and the MTs removed by centrifugation [Andersen et al., 1994]. As an alternative to the Andersen et al. [1994] protocol, MAPs were prepared from extracts diluted with 1 vol cold CSF-XB (see preparation of extracts) by addition of approximately 5 µM (tubulin-equivalent) taxol stabilized MTs plus 20 µM taxol, followed by 10-min incubation on ice and isolation through sucrose cushions [Andersen et al., 1994] containing 1 µM micro-cystin. Both types of MAP preparations gave similar results. Note that during the experiments described here, MAPs were prepared from freshly prepared extracts and used for the video assay on the same day without freezing. When extracts or MAPs were frozen, there was a 1.5– to 3-fold reduction in the effect on MT growth rate.

Desalting of MAPs

MAPs were desalted on a Fast Desalting PC 3.2/10 column (SMART, Pharmacia LKB Biotechnology, Uppsala, Sweden) at 4°C, pre-equilibrated with CSF-XB (for bulk polymerization assay; Fig. 4) or with BRB80 (for video microscopy experiments, Fig. 5; BRB80: 80 mM K-pipes, 1 mM $MgCl_2$, 1 mM EGTA, pH = 6.8). After desalting of the MAPs the total protein concentration was measured by Bradford with bovine serum albumin (BSA) as the standard.

Bulk Microtubule Assembly Assay

In this assay, pure tubulin (40 µM final in BRB80 and 1 mM GTP final) was mixed on ice with MAPs or control buffer (CSF-XB) and the mix transferred to a 1-cm Quartz-cuvette (Hellma #105.202-QS; the same total amount of I and M MAPs were used, and typically constituted 1/15 of the total volume (60 µl) of the bulk assembly reaction). The cuvette was then shifted to 37°C and the increase in turbidity at 350 nm recorded 20 times/min using a Uvikon 930 Spectrophotometer (Kontron Instruments, Tegimenta, Rotkreuz Switzerland) [Gaskin et al., 1974; Voter and Erickson, 1984]. The data were plotted using Kaleidagraph 3.0, and curve-averaging performed with Microsoft Excel 5.0.

Video Microscopy

Double-sided tape chambers with a volume of ~3–4 µl were used [Andersen and Karsenti, 1997]. The channel formed by the tape strips, the slide and the coverslip made up the chamber. Before use, centrosomes (3×10^3/µl) with 20 µM tubulin were injected into the chamber and left for 5 min on ice. MAPs desalted into BRB80 were then diluted into concentrated tubulin and the mix adjusted to 40 µl, 20 µM tubulin, 1 mM GTP by the addition of BRB80 and Mg-GTP (50 mM stock). By capillary forces, the chamber was washed with the 40-µl sample and placed on the stage of a video microscope heated to 25°C. Measurements of MT dynamics were performed as described [Andersen et al., 1994].

^{32}P-Labeling of MAPs

Undiluted 100,000*g* extracts were incubated with 5 µM pre-polymerized taxol stabilized MTs and 10 µM taxol for 15 min at room temperature, followed by 10-min labeling with 1 µCi [γ-^{32}P]ATP/µl extract, and MAP preparation and elution as described above. Measure-

ments of the PP1 and PP2A phosphatase activities in the MAP pellets, with and without micro-cystin treatment, were performed as described by [Tournebize et al., 1997].

Calculations

The curves shown in Figure 3 were derived using the equation shown below [Andersen et al., 1994]. K_d is the molar dissociation constant of MAP from MTs, mx is the molar concentration of the complex between MTs (m) and MAP (x), m is the total molar concentration of tubulin polymerized into MTs and x is the total molar concentration of MAP:

$$mx = \frac{1}{2}(K_d + m + x) - \sqrt{\frac{1}{4}(K_d + m + x)^2 - m \cdot x} \quad (1)$$

To calculate the curves shown in Figure 3, the total molar concentration of MAP was set to 200 nM, which is in the range of the estimated in vivo concentration of XMAP230 and XMAP310 [Andersen et al., 1994; Andersen and Karsenti, 1997]. For different constant values of K_d (0.5, 5 or 10 μM) the value of m was varied and mx calculated. Note that this calculation assumes a simple 1:1 MAP-tubulin binding stoichiometry, and that the MAP binds homogenously along the entire length of the MTs. Thus, for factors that bind specifically to the minus- or plus- end of MTs this approximation can not be used. Examples of such factors are γ-tubulin at the minus-end [Li and Joshi, 1995] and probably XMAP215 at the plus-end (S.K. Jain, A. Popov, T.J. Mitchison, A. Podtelejnikov, S.S.L. Andersen, A.J. Ashford, M. Mann, and A.A. Hyman, unpublished observations).

Miscellaneous

Calf brain tubulin was prepared by two cycles of polymerization and depolymerization, phosphocellulose chromatography and subsequently cycling and storage in N_2(1) [Ashford et al., 1998; Mitchison and Kirschner, 1984a]. Human centrosomes were prepared from KE37 lymphoblasts according to Bornens et al. [1987]. Unless otherwise indicated, chemicals were from Sigma Chemical Co. (St. Louis, MO), or Boehringer Mannheim (Mannheim, Germany).

RESULTS

Purification and Microtubule Binding of Interphase and Mitotic MAPs

To identify molecules with affinity for MTs, taxol was added to *Xenopus* egg extracts to induce MT polymerization [Andersen et al., 1994; Vallee, 1982]. The tubulin concentration in the eggs is on the order of 20 μM (2 mg/ml) [Houliston and Elinson, 1992; Zhai et al., 1996], and this endogenous tubulin polymerized in the presence of 20 μM taxol in both interphase (I) and mitotic (M) extracts (data not shown). In order to (1) ensure good depletion of MAPs, and (2) improve the reproducibility of depletion, 5 μM exogenous prepolymerized taxol stabilized bovine brain MTs was also added to the extracts. After incubation of the MTs in the extract, MTs were recovered by centrifugation through two 40% sucrose cushions [Andersen et al., 1994]. To prevent dephosphorylation during the purifications and preserve the phosphorylation level of the MAPs, 1 μM micro-cystin was added to the sucrose cushions during the purification. Measurements showed that this treatment irreversibly inhibited the PP1 and PP2A phosphatase activities present in the MT-MAP fractions (data not shown). Conversely, as there is no ATP in the sucrose cushion, phosphorylation of MAPs by MT-associated kinases does not occur once the MAPs are in the sucrose cushion. The MAPs were eluted from the MT pellet with 400 mM NaCl in BRB80 plus taxol, and the MTs removed by centrifugation.

Analysis by sodium dodecyl sulfate polyacrylamide gel electrophoresis (SDS-PAGE) of the eluted MAPs revealed that 20–40 proteins bind to MTs in I and M extracts, and that the pattern of MAPs is similar between I and M (Fig. 1a). From these experiments, the total MAP concentration was estimated at 500 μg/ml extract, or roughly 0.5% of the total extract proteins. Since ATP was not depleted from the extract before MAP purification, the MAP fraction, referred to as ''total MAPs'' in this report, is devoid of activities like motor proteins. Note also that the purpose of the investigation was to study the population of proteins co-purifying with MTs in a crude extract, rather than only so-called bona fide/structural MAPs (purified proteins able to bind pure MTs). However, the majority of the proteins in Figure 1 a were able to rebind to MTs after desalting, indicating that most of the proteins in Figure 1 a are bona fide MAPs (data not shown) [Faruki and Karsenti, 1994]. Interestingly, the addition of the 5–10 μM exogenous pre-polymerized taxol stabilized MTs was sufficient to bind the MAPs, as no quantitative differences were observed as to whether the endogenous pool of tubulin was also polymerized before MAP preparation (data not shown).

Previous reports indicate that several individual MAPs bind less tightly to MTs in M compared with I. It was therefore investigated to what extent this observation applied to total I and M MAPs in concentrated 100,000*g* extract in the presence of 5–10 μM prepolymerized MTs. While the overall pattern is similar, there was in particular a reduction in the MT binding of MAPs of >200 kDa in M compared with I extracts (Fig. 1a, 4%). At <200 kDa

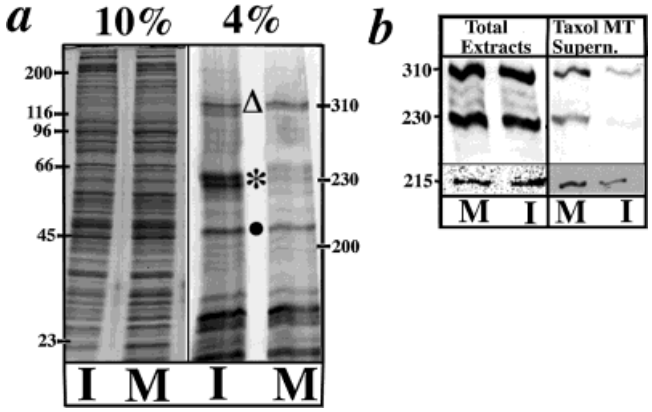

Fig. 1. **a:** Representative patterns of microtubule-associated proteins (MAPs) from interphase (I) and mitotic (M) *Xenopus* egg extracts. MAPs from equivalent volumes of I and M extracts were resolved by 4% and 10% Coomassie-stained sodium dodecyl sulfate polyacrylamide gel electrophoresis (SDS-PAGE) (routinely 10% less MTs were recovered from M compared with I extracts and loadings were normalized accordingly); ●, XMAP215 [Charasse et al., 1998; Gard and Kirschner, 1987; Vasquez et al., 1994], *, XMAP230 [Andersen et al., 1994), and △, XMAP310 [Andersen and Karsenti, 1997]. **b:** Western blot of 4% SDS-PAGE with anti-XMAP215 (215), anti-XMAP230 (230) and anti-XMAP310 (310) antibodies from interphase (I) and mitotic (M) extracts. Total extracts is the starting extract before depletion. Taxol MT supernatant is the extract after depletion of MAPs. Molecular mass markers are indicated.

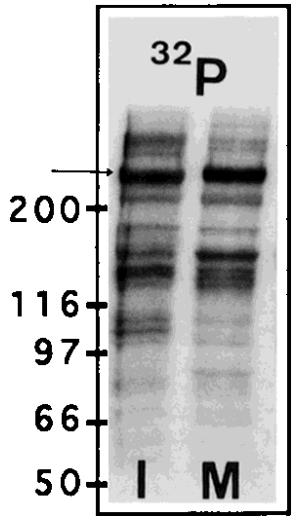

Fig. 2. Representative autoradiogram of ^{32}P-labeled microtubule-associated proteins (MAPs) prepared after addition of [γ-^{32}P]ATP to concentrated 100,000*g* interphase (I) and mitotic (M) *Xenopus* extracts. *Arrow*, XMAP230. 6% sodium dodecyl sulfate polyacrylamide gel electrophoresis (SDS-PAGE). Molecular mass markers are indicated.

the pattern of bound proteins is complex and only minor differences can be observed between I and M. In order to get an estimate for the reduction in binding activity of MAPs between I and M, the three currently characterized MAPs from *Xenopus* were studied: XMAP215 [Charasse et al., 1998; Gard and Kirschner, 1987; Vasquez et al., 1994], XMAP230 [Andersen et al., 1994; Andersen and Karsenti, 1998; Shiina et al., 1992], and XMAP310 [Andersen and Karsenti, 1997]. Western blotting showed that XMAP310 and XMAP230 showed an approximately 40% reduction in binding capacity in M compared with I extracts (Fig. 1b). Moreover, XMAP215 also show reduced binding to MTs in M extracts, but not as pronounced as XMAP230 and XMAP310. These data indicate that some, but not all, MAPs bind less tightly to MTs during M (it is currently not possible to extend this analysis because no additional antibodies are available against *Xenopus* MAPs).

To check whether there were any differences in the phosphorylation pattern of I and M MAPs, extracts were labeled with [γ-^{32}P]ATP and MAPs prepared. Although there were differences, the ^{32}P pattern of I and M MAPs was surprisingly similar (Fig. 2). Interestingly, some proteins were more phosphorylated in I than in M. The reverse was also observed, and in particular XMAP230 showed a pronounced phosphorylation dependent shift in molecular weight from I to M, as previously reported [Andersen et al., 1994; Shiina et al., 1992]. Analysis by two-dimensional gel electrophoresis did not show any MAP, apart from XMAP230, that was in particular differentially phosphorylated between I and M (data not shown).

The [γ-^{32}P]ATP gel in Figure 2 measures absolute amounts of radioactivity present on any one protein. Therefore, since some proteins, and in particular XMAP230, bind less to MTs in M compared with I extracts (Fig. 1) but still give rise to a similar ^{32}P signal, it is inferred that these MT associated MAPs are more phosphorylated in M than I. Since phosphorylation previously has been shown to lower the affinity of MAPs, it may at first seem peculiar that highly phosphorylated MAPs like XMAP230 are MT associated. However, this simply reflects that the highly phosphorylated M form of XMAP230 has lower affinity/higher dissociation constant (K_d) from MTs than the I form. A rough estimation of the change in K_d can be derived from the theoretical curves shown in Figure 3. The curves were derived using equation 1 in materials and methods, and shows that the residual 60% XMAP230 binding observed in M extracts corresponds roughly to a 10-fold increase K_d between I and M.

These data suggest that some, but not all, MAPs bind less tightly to MTs in M compared with I. The lack of massive phosphorylation of M MAPs indicates that the changes in binding activity between I and M may be due to minor site-specific differences in MAP phosphorylation between I and M, as opposed to global phosphorylation of the entire protein [Illenberger et al., 1996].

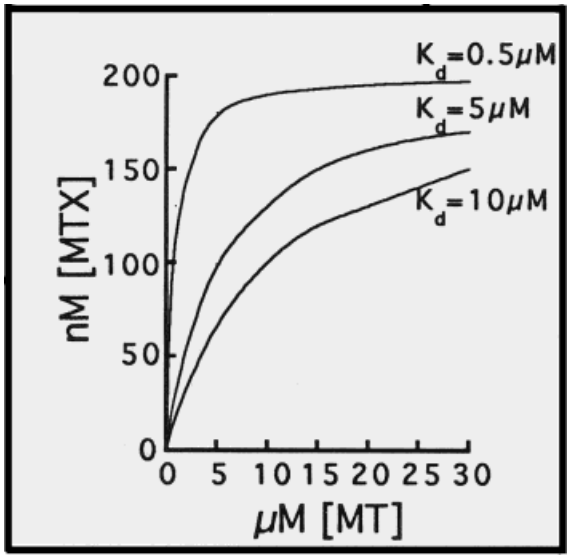

Fig. 3. Theoretical graph showing the concentration of microtubule–microtubule-associated protein (MT-MAP) complex formed [MTX] as a function of the concentration of tubulin polymerized into MTs [MT] and the dissociation constant (K_d) of the MAP from MTs (see under Materials and Methods, Eq. 1). The theoretical graph shows that at 15 μM MTs, 200 nM MAP concentration, and a K_d of 0.5 μM (approximate conditions for XMAP230 and XMAP310 in I extracts) all MAP would be MT bound, and this was what was experimentally observed for both XMAP230 and XMAP310 in I extracts. It is seen from the graph that the measured approximately 60% binding of XMAP230 and XMAP310 to MTs in M extracts corresponds to a 10- to 20-fold increase in K_d (for a [MTX] = 120 nM K_d = 5–10 μm) compared with I extracts.

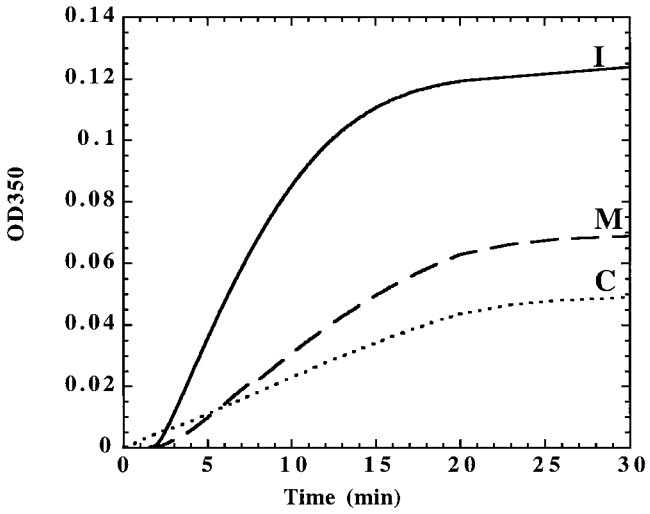

Fig. 4. Bulk polymerization of microtubules (MTs) in the presence of interphase (I) or mitotic (M) microtubule-associated proteins (MAPs) or control buffer (C). Desalted (into CSF-XB) total I and M MAPs (at 150 μg/ml final concentration) were mixed with 40 μM (final concentration) pure tubulin, 1 mM GTP, and bulk polymerization at 37°C, followed with time at 350 nm (20 recordings/min). Curves are averages of two experiments. Note: these experiments were not designed to determine how MAPs affect MT nucleation.

Bulk Microtubule Polymerization

The next step in the characterization of the total I and M MAPs consisted of a rough comparison of their ability to induce MT polymerization. Thus, the aim was to see whether M MAPs are less potent MT stabilizers than I MAPs, despite the similar molecular composition and phosphorylation levels. To this end, the MAPs in Figure 1 were desalted and their effect on bulk MT polymerization observed (Fig. 4). In this assay pure tubulin and GTP is on ice mixed with the same amount of total I or M MAPs or control buffer, then shifted to 37°C and the spontaneous assembly, followed at 350 nm. The increase in turbidity at 350 nm correlates with the amount of MTs assembled, and the kinetic increase in turbidity can be used as a measure of the relative potency of MAPs and other molecules for MT assembly [Gaskin et al., 1974; Voter and Erickson, 1984]. In order to obtain measurable assembly, it was necessary to perform these experiments at 37°C and with 40 μM tubulin.

At the same tubulin and total MAP concentration, both I and M MAPs promoted MT assembly compared to control buffer (Fig. 4, I and M compared with C). However, in the presence of I MAPs there was approximately a two-fold increase in the slope of the curve compared with M MAPs during the growth phase. This result indicates that I MAPs cause MTs to polymerize two times faster than M MAPs (Fig. 4, I and M). At steady-state (Fig. 4, flat part of the curve), the tubulin concentration has dropped to a level that does not allow a further increase in the total MT mass. However, these MTs remain dynamic and also undergo treadmilling [Hotani and Hori, 1988; Mitchison and Kirschner, 1984]. Thus, at steady-state there is equilibrium between the tendency of the MTs to depolymerize and to continue polymerization. Since the steady-state level of MT polymerization is approximately twofold higher in the presence of I compared with M MAPs indicates that I MAPs are more potent than M MAPs at inducing MT polymerization (Fig. 4, I and M). These data show that I MAPs are roughly twofold stronger at promoting MT assembly as compared to their M counterparts.

Microtubule Dynamics Observed by Video Microscopy

To confirm the data obtained by the bulk polymerization assay (Fig. 4) and to get a more detailed picture of the effect, it was measured how I and M MAPs affect MT dynamics by time-lapse video microscopy (Fig. 5a,b). In this assay, MTs are nucleated by centrosomes (Andersen, 1999b) and MT dynamics followed by time lapse video microscopy (Fig. 5a), as previously described [Andersen et al., 1994; Andersen and Karsenti, 1997]. This assay

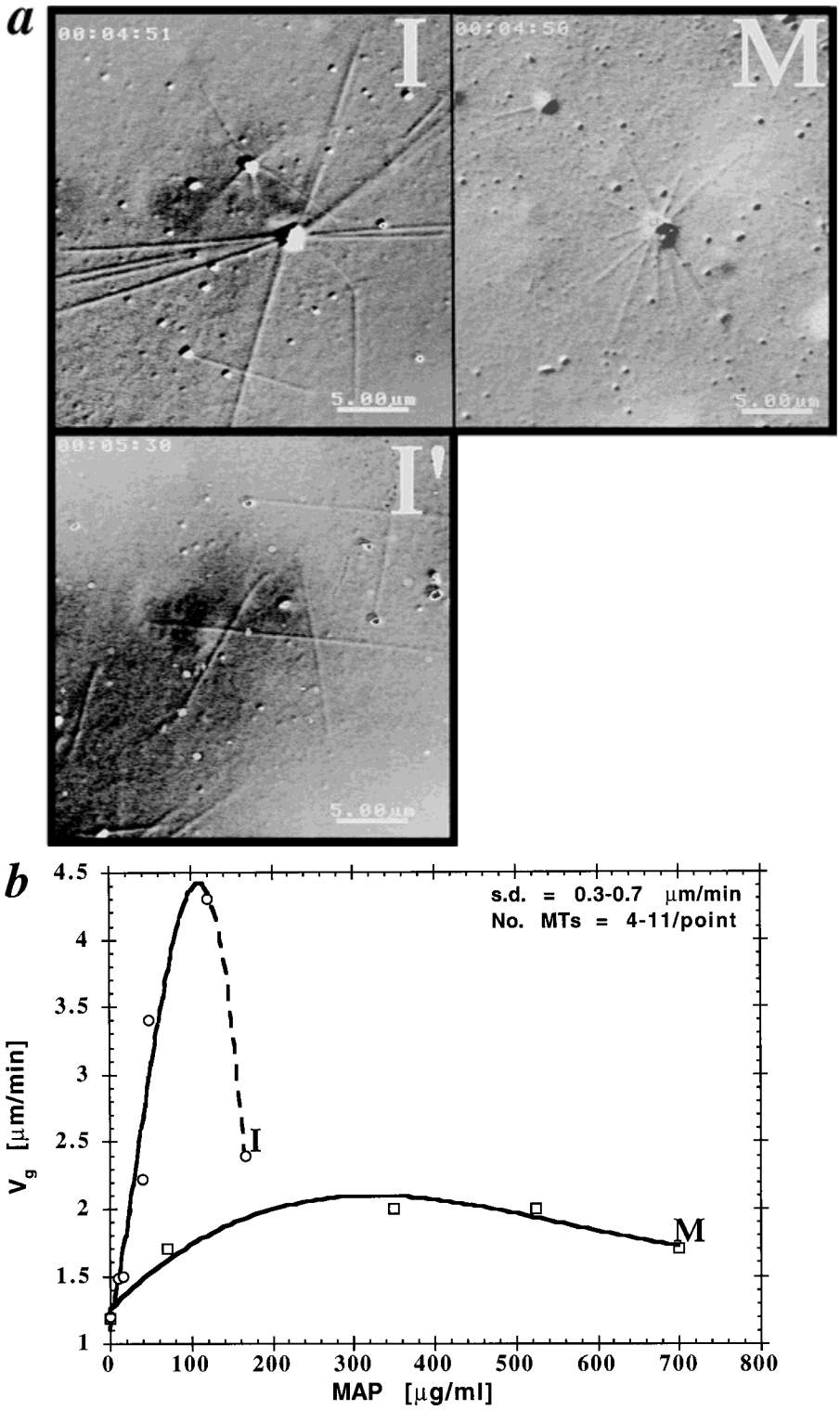

Fig. 5. Growth rate of pure centrosome-nucleated MTs as a function of the concentration of total interphase (I) and mitotic (M) *Xenopus* MAPs (desalted into BRB80). **a:** MTs grown off centrosomes in the presence of I (83 µg/ml) and M (420 µg/ml) *Xenopus* MAPs; I shows an I MT aster after 00 h : 04 min : 51 s of growth, and M an mitotic MT aster after 00 h : 04 min : 50 s of growth; I′ shows a field with spontaneously assembled MTs in the presence of I MAPs at 00 h : 0.5 min : 30 s; No spontaneous assembly was observed in the presence of M MAPs (data not shown). Bar = 5 µm. **b:** MT growth rates (V_g) as a function of the concentration of total desalted I and M MAPs (MAP [µg/ml]); The stippled line indicates the drop in v_g noted at higher I MAP concentrations; The experiments were performed with 20 µM tubulin in BRB80, 1 mM GTP (the in vivo tubulin concentration is 20 µM [Houliston and Elinson, 1992; Zhai et al., 1996]) and at 25°C (at higher temperatures MTs grew too fast for measurements to be possible); For each point, 4–11 MTs were measured (No. of MTs) and the standard deviation (SD) was 0.3–0.7 µm/min (top right corner). A total of 28 I MTs (34-min observation time) were measured, and 37 (61-min observation time) for the M MAPs. Three different batches of I and three different batches of M MAPs were used for these experiments.

was performed with 20 μM tubulin (the concentration in the extract) and at 25°C, since at 37°C MTs polymerized too fast for proper MT dynamics measurements to be possible and *Xenopus* frogs live at around 25°C. However, at 25°C and 20 μM tubulin pure MTs do not polymerize, and measurement of the dynamics of pure MTs was therefore not performed.

At fixed tubulin concentration the concentration of total MAPs was varied (Fig. 5b; x-axis). The experiments were performed in a MAP concentration range matching the estimated in vivo concentration of 500 μg MAP/ml extract. 28 MTs were measured for I MAPs and 37 MTs were measured for M MAPs. Interestingly, none of these MTs ever experienced a catastrophe event. Since the MTs never underwent catastrophes, there were no shrinking events and therefore no rescues. Thus, the only measurable dynamic parameter was growth rate (v_g), and a graphic representation of v_g as a function of MAP concentrations is shown in Fig. 5b, I and M. The experiments show that the maximal growth rate in the presence of I MAPs was twofold higher than with M MAPs (Fig. 5b).

In the presence of high concentrations of I MAPs massive centrosome-independent MT polymerization made measurements of individual MTs impossible (Fig. 5b, I, beyond the stippled line). Moreover, in the presence of I MAPs, there was a drop in v_g at MAP concentrations beyond the concentration of MAPs that resulted in maximal v_g (Fig. 5b, I, stippled line). This drop in v_g is most likely caused by the induction of spontaneous MT nucleation and assembly by the I MAPs (Fig. 5a, I′), which will cause the tubulin concentration to drop rapidly and thereby decrease v_g (Fig. 5b, I, stippled line). Interestingly, the strong spontaneous nucleation occurred already at MAP concentrations below the estimated in vivo concentration. In the presence of M MAPs, no spontaneous MT assembly was ever observed, and the growth rate remained constant at MAP concentrations beyond the concentration of M MAPs that resulted in maximal MT growth rate (Fig. 4b, M).

These data show that both total I and M MAPs suppress MT dynamics by eliminating catastrophes. Total I MAPs promote growth twofold more than total M MAPs. Interestingly, I MAPs strongly promoted spontaneous assembly whereas M MAPs did not.

DISCUSSION

The mechanism underlying the change in MT dynamics at the interphase (I) to mitosis (M) transition is still largely unknown. The hallmark of the change in MT dynamics is an increased f_{cat} in M compared with I extracts [Belmont et al., 1990; Parsons and Salmon, 1997; Tournebize et al., 1997; Verde et al., 1992]. To explain this change in dynamics, it has been hypothesized that a ''catastrophe factor'' is specifically activated at the onset of M [i.e., Belmont et al., 1996]. The definition of a bona fide catastrophe factor is a molecule that is specifically activated during M and induces MT catastrophes either directly or indirectly. However, no such factor has yet been identified, as further discussed below. An alternative hypothesis is that the balance between MT destabilizing (like XKCM1 and Stathmin/Op18) and stabilizing factors (e.g., MAPs) at any time and spatial point during the cell cycle controls the dynamic state of the MTs [Andersen, 1999a]. To probe this possibility, this study investigated whether there are any differences in the effect on MT dynamics of total MAPs from I and M extracts. For example, it was possible that these two fractions of MAPs would affect MT dynamics in the same way, or perhaps the M MAPs would contain a factor that could render MTs dynamic.

Toward Reconstitution of In Vivo Microtubule Dynamics In Vitro

Interestingly, this report shows that isolated total I and M MAPs affect MT dynamics differently. The question is then how closely the I and M MAP fractions mimic the dynamics of MTs observed during I and M in *Xenopus* egg extracts?

In I *Xenopus* egg extracts, there is rapid spontaneous MT nucleation and assembly, and catastrophe events are rare. In contrast, in M extracts there is no spontaneous MT assembly, f_{cat} is roughly 10-fold higher than in I and the v_g approximately twofold lower than in I [Belmont et al., 1990; Parsons and Salmon, 1997; Tournebize et al., 1997; Verde et al., 1992]. Thus, the direct observation by video microscopy that induction of MT nucleation is strongly stimulated by I compared with M MAPs fits with the situations in the I and M extracts. While it is possible that the nucleation of free I MTs in vivo is under the control of the γ-TuRC [Dictenberg et al., 1998], this study shows that total I MAPs can strongly promote MT nucleation. It seems likely that I MAPs contribute to the formation of free cytoplasmic MTs during I [Vorobjev et al., 1997]. It is also worth noting that these somatic MAPs do not support MT nucleation as potently as neuronal MAPs. This argues that proteins like the brain MAP tau, that very strongly induces MT nucleation, are absent from these non-neuronal MAPs. The twofold difference in maximal v_g between I and M MAPs corresponds well to the relative difference between v_gs observed in I and M *Xenopus* egg extracts. Therefore, upon addition of the total I and M MAP fractions to MTs in vitro, some of the properties of MT dynamics in I and M extracts are reconstituted.

The most important missing dynamic instability parameter in this reconstituted system is the complete

lack of catastrophes in the presence of both I and M MAPs. Since pure control MTs did not polymerize at the 25°C, 20 μM tubulin used, both I and M MAPs potently promote MT assembly and suppress MT dynamics. The most likely reason for the absence of catastrophes is that factors such as XKCM1 and Stathmin/Op18 that do not bind to MTs under the conditions used, but destabilize MTs and probably make MTs dynamic in vivo, are not represented in this system [Belmont and Mitchison, 1996; Curmi et al., 1997; Sobel, 1991; Walczak et al., 1996].

One may argue that the different effects on MT dynamics of I and M MAPs are caused by one specific MAP (i.e., XMAP230). While this possiblity can not be excluded it seems unlikely. For example, since it is known that XMAP215 enhances plus-end microtubule assembly 10-fold [Vasquez et al., 1994], compared with the two- to fourfold enhancement by XMAP230 [Andersen et al., 1994], the slight reduction of XMAP215 in the total M MAP fraction could also explain some of the differences in the effect of MAPs on MT assembly between I and M. It seems fair to say that there are differences between the effect of I and M MAPs on MT assembly but the precise molecular basis for these differences remains to be clarified. Moreover, the purpose of this study was to test the activity differences between total I and M MAPs. Such an experiment more closely mimic the extract and the in vivo situation than studies considering the effect of a single MAP on MT dynamics. It is also important to note that the total MAP concentrations used in this study (<700 μg/ml) are in the range of the estimated 500 μg MAP/ml extract, and therefore biologically relevant. Interestingly, there is not a big difference in the composition or phosphorylation patterns between I and M MAPs, despite their different effects on MT dynamics. This may indicate that rather than global phosphorylation of MAPs, the activity of MAPs is regulated by site-specific phosphorylation that cannot be resolved with the techniques used here [Drewes et al., 1997; Illenberger et al., 1996]. More work is clearly needed to resolve how the total I and M MAPs differentially promote MT polymerization.

MAPs as Regulators of Microtubule Dynamics

The results suggest that regulation of MAP activity may be the switch that regulate MT dynamics from I to M. How could regulation of MAPs regulate the change in MT dynamics from I to M in vivo? Let us now imagine that regulation of the balance between MT stabilizing (MAPs) and destabilizing activities lies at the heart of MT dynamics regulation in vivo.

Looking at the large amounts of MAPs co-pelleting with MTs (Fig. 1), it seems likely that MTs in vivo are saturated with MAPs. Therefore, these MAPs are competing with each other and with destabilizing factors for interaction with the MT lattice. In I, these MAPs are dephosphorylated and bind tightly (nM range) to MTs, while in M, the MAPs are more phosphorylated and their affinity for MTs drop at least 10-fold (this study; and [Andersen et al., 1994; Drechsel et al., 1992; Masson and Kreis, 1995; Olmsted et al., 1989; Shiina et al., 1992]. Interestingly, M MAPs are 2-fold less potent than I MAPs at promoting MT assembly but still suppress MT dynamics even under conditions (25°C, 20 μM tubulin), where pure MTs are very dynamic. This decreased affinity and MT stabilizing activity of M compared to I MAPs may well be the switch that allows destabilizing factors (i.e., XKCM1 and Stathmin/Op18) to induce MT catastrophes, by overcoming the residual stabilizing effect of the M MAPs. Thus, if the activity of MT destabilizing factors is constant during the cell cycle, control of the activity of stabilizing factors could regulate the dynamic state of MTs.

What is known about cell cycle regulation of MT destabilizing factors? The phosphorylation level of Stathmin/Op18 does not change between I and M in *Xenopus* egg extracts [Andersen et al., 1997]. Since it is the dephosphosphorylated form that destabilizes MTs, Stathmin/Op18 is constitutively active during the cell cycle. Thus, cell cycle regulation of Stathmin/Op18 activity/phosphorylation is not, as previously proposed, responsible for the increase in f_{cat} between I and M [Belmont et al., 1996; Curmi et al., 1997; Horwitz et al., 1997; Larsson et al., 1997; Marklund et al., 1996]. Moreover, recent in vitro experiments show that Stathmin/Op18 does not induce MT catastrophes in vitro but destabilizes MTs by sequestering tubulin [Curmi et al., 1997; Jourdain et al., 1997]. The motor XKCM1 induces catastrophes, even when added to taxol MTs. However, the available data suggest that there is no differential regulation of XKCM1 activity between I and M [Walczak et al., 1996]; therefore, this protein also does not qualify as a bona fide catastrophe factor. Therefore, it appears that MT destabilizing factors are constitutively active during the cell cycle.

Since destabilizing factors apparently are constitutively active, regulation of the activity of the (dominant) stabilizing factors could function as a switch regulating the change in MT dynamics at the I to M transition [Andersen, 1999a]. It will be interesting to test this hypothesis and to gain more insight into the cell cycle regulation of MT destabilizing factors.

Reconstitution of In Vivo Microtubule Dynamics In Vitro

The next steps towards reconstitution of in vivo MT dynamics in vitro will involve addition of molecules like Stathmin/Op18 [Belmont and Mitchison, 1996], XKCM1 [Walczak et al., 1996] and severing factors [i.e., Hartman et al., 1998; Vale, 1991] to the mix of tubulin, centrosomes, and total MAPs. It will be exciting to determine the amounts necessary to observe catastrophes in the

presence of MAPs. Ultimately, a more defined reconstituted system requires identification of the core components that can reproduce in vitro the MT dynamics phenomenon observed in vivo during I and M. An interesting approach will be to deplete MAPs from both extracts and MAP fractions and monitor how this affects the dynamics of the extract MTs and the pure MTs. Such an approach may be valuable for the determination of core MAPs.

In addition to stabilizing and destabilizing factors as well as kinases and phosphatases, other factors and regulation mechanisms are perhaps required to make MTs dynamic. For example, the tubulin isotype and buffer composition influence MT dynamics [Haber et al., 1995; Moore et al., 1997; Panda et al., 1994; Simon et al., 1992]. While these factors are important for MT dynamics in vitro they are most likely minor factors in vivo, where MAPs and destabilizing factors probably are dominant. Little is known about global and local [Zhai et al., 1996] regulation of the free tubulin pool in vivo, although this parameter strongly affects MT dynamics in vitro [Fygenson et al., 1994; Parsons and Salmon, 1997; Walker et al., 1988]. Moreover, early studies indicated that regulation of the concentration of oxidized glutathione/redox potential has dramatic effects on MTs in vivo [Oliver, 1978].

However, it seems most likely that the dynamic state of MTs is regulated by a balance between the activity of proteinatious MT stabilizing and destabilizing factors [Andersen, 1999a]. With our present understanding of MT dynamics regulation the stage is set for an exciting complete reconstitution of in vivo MT dynamics in vitro.

ACKNOWLEDGMENTS

I am grateful to David Gard (University of Utah) for the gift of the XMAP215 antibody and to the EMBL where this work was carried out. Special thanks to Anthony Ashford, Anthony Hyman, and Fedor Severin for mutual pleasure during the purifications of bovine brain tubulin.

REFERENCES

Andersen, S.S.L. (1999a): Balanced regulation of microtubule dynamics during the cell cycle: A contemporary view. BioEssays (in press).

Andersen, S.S.L. (1999b): Molecular characteristics of the centrosome. Int Rev Cytol. 187 (in press).

Andersen, S.S.L. (1995): A functional assay for the identification and characterization of microtubule-associated proteins involved in the regulation of microtubule dynamics and mitotic spindle assembly. Dissertation, European Molecular Biology Laboratory/ Heidelberg University, Germany, 157 pp.

Andersen, S.S.L., and Karsenti, E. (1997): XMAP310: a *Xenopus* rescue promoting factor localized to the mitotic spindle. J Cell Biol. 139:975–983.

Andersen, S.S.L., and Karsenti, E. (1998): XMAP230. In Kreis T., and Vale, R. (eds): ''Guidebook to the Cytoskeleton and Motor Proteins.'' (in press).

Andersen, S.S.L., Buendia, B., Domínguez, J.E., Sawyer, A., and Karsenti, E. (1994): Effect on microtubule dynamics of XMAP230, a microtubule-associated protein present in *Xenopus laevis* eggs and dividing cells. J. Cell Biol. 127:1289–1299.

Andersen, S.S.L., Ashford, A.J., Tournebize, R., Gavet, O., Sobel, A., Hyman, A.A., and Karsenti, E. (1997): Mitotic chromatin regulates phosphorylation of Stathmin/Op18. Nature 389:640–643.

Andreassen, P.R., Lacroix, F.B., Villa-Moruzzi, E., and Margolis, R.L. (1998): Differential subcellular localization of protein phosphatase-1 alpha, gamma1, and delta isoforms during both interphase and mitosis in mammalian cells. J Cell Biol. 141:1207–1215.

Ashford, A.J., Andersen, S.S.L., and Hyman, A.A. (1998): Purification of bovine brain tubulin. In Celis, J.E. (ed.): ''Cell Biology: A Laboratory Handbook.'' San Diego: Academic Press, pp. 205–212.

Belmont, L., Mitchison, T., and Deacon, H.W. (1996): Catastrophic relevations about Op18/stathmin. Trends Biochem Sci 21:197–198.

Belmont, L.D., and Mitchison, T.J. (1996): Identification of a protein that interacts with tubulin dimers and increases the catastrophe rate of microtubules. Cell 84:623–631.

Belmont, L.D., Hyman, A.A., Sawin, K.E., and Mitchison, T.J. (1990): Real-time visualization of cell cycle-dependent changes in microtubule dynamics in cytoplasmic extracts. Cell 62:579–589.

Billger, M.A., Bhatacharjee, G., and Williams, R.C. (1996): Dynamic instability of microtubules assembled from microtubule-associated protein-free tubulin: Neither variability of growth and shortening rates nor ''rescue'' requires microtubule-associated proteins. Biochemistry 35:13656–13663.

Bornens, M., Paintrand, M., Berges, J., Marty, M.C., and Karsenti, E. (1987): Structural and chemical characterization of isolated centrosomes. Cell Motil. Cytoskeleton 8:238–249.

Bré, M.H., and Karsenti, E. (1990): Effects of brain microtubule-associated proteins on microtubule dynamics and the nucleating activity of centrosomes. Cell Motil. Cytoskeleton 15:88–98.

Bulinski, J.C., McGraw, T.E., Gruber, D., Nguyen, H.L., and Sheetz, M.P. (1997): Overexpression of MAP4 inhibits organelle motility and trafficking in vivo. J Cell Sci. 110:3055–3064.

Burns, R.G., Islam, K., and Chapman, R. (1984): The multiple phosphorylation of the microtubule-associated protein MAP2 controls the MAP2:tubulin interaction. Eur J Biochem. 141:609–615.

Cassimeris, L., Pryer, N.K., and Salmon, E.D. (1988): Real time observations of microtubule dynamic instability in living cells. J. Cell Biol. 107:2223–2231.

Charasse, S., Schroeder, M., Gauthier-Rouviere, C., Ango, F., Cassimeris, L., Gard, D.L., and Larroque, C. (1998): The TOGp protein is a new human microtubule-associated protein homologous to the Xenopus XMAP215. J. Cell Sci. 111:1371–1383.

Chrétien, D., Fuller, S.D., and Karsenti, E. (1995): Structure of growing microtubule ends: two-dimensional sheets close into tubes at variable rates. J Cell Biol. 129:1311–1328.

Cleveland, D.W., Fischer, M.W., Kirschner, M.W., and Laemmli, U.K. (1977): Peptide mapping by limited proteolysis in sodium dodecyl sulfate and analysis by gel electrophoresis. J. Biol. Chem. 252:1102–1106.

Curmi, P.A., Andersen, S.S.L., Lachkar, S., Gavet, O., Karsenti, E., Knossow, M., and Sobel, A. (1997): The Stathmin/tubulin interaction in vitro. J Biol Chem. 272:25029–25036.

Dhamodharan, R., and Wadsworth, P. (1995): Modulation of microtubule dynamic instability in vivo by brain microtubule associated proteins. J Cell Sci. 108:1679–1689.

Dictenberg, J.B., Zimmerman, W., Sparks, C.A., Young, A., Vidair, C., Zheng, Y., Carrington, W., Fay, F.S., and Doxsey, S.J. (1998): Pericentrin and γ-tubulin form a protein complex and are organized into a novel lattice at the centrosome. J Cell Biol. 141:163–174.

Drechsel, D.N., Hyman, A.A., Cobb, M.H., and Kirschner, M.W. (1992): Modulation of dynamic instability by the microtubule-associated-protein tau. Mol. Biol. Cell. 3:1141–1154.

Drewes, G., Ebneth, A., Preuss, U., Mandelkow, E.-M., and Mandelkow, E. (1997): MARK, a novel family of protein kinases that phosphorylate microtubule-associated proteins and trigger microtubule disruption. Cell 89:297–308.

Faruki, S., and Karsenti, E. (1994): Purification of microtubule proteins from *Xenopus* egg extracts: Identification of a 230K MAP4-like protein. Cell Motil. Cytoskeleton 28:108–118.

Félix, M.A., Clark, P., Coleman, J., Verde, F., and Karsenti, E. (1994): Frog egg extracts as a system to study mitosis. In Fantes, P. (ed.): ''The Cell Cycle: A practical Approach.'' New York: IRL Press, pp. 253–283.

Fygenson, D.K., Braun, E., and Libchaber, A. (1994): Phase-diagram of microtubules. Phys. Rev. E 50:1579–1588.

Gard, D., and Kirschner, M. (1987): A microtubule-associated protein from *Xenopus* eggs that specifically promotes assembly at the pluse end. J Cell Biol. 105:2203–2215.

Gaskin, F., Cantor, C.R., and Shelanski, M.L. (1974): Turbidimetric studies of the in vitro assembly and disassembly of porcine neurotubules. J. Mol. Biol. 89:737–758.

Gliksman, N.R., Parsons, S.F., and Salmon, E.D. (1992): Okadaic acid induces interphase to mitotic-like microtubule dynamic instability by inactivating rescue. J. Cell Biol. 119:1271–1276.

Gliksman, N.R., Skibbens, R.V., and Salmon, E.D. (1993): How the transition frequencies of microtubule dynamic instability (nucleation, catastrophe, and rescue) regulate microtubule dynamics in interphase and mitosis: Analysis using a Monte Carlo computer simulation. Mol. Biol. Cell. 4:1035–1050.

Glotzer, M., Murray, A.W., and Kirschner, M.W. (1991): Cyclin is degraded by the ubiquitin pathway. Nature 349:132–138.

Gotoh, Y., Nishida, E., Matsuda, S., Shiina, N., Kosako, H., Shiokawa, K., Akiyama, T., Ohta, K., and Sakai, H. (1991): In vitro effects on microtubule dynamics of purified *Xenopus* M phase-activated MAP kinase. Nature 349:251–254.

Haber, M., Burkhart, C.A., Regl, D.L., Madafiglio, J., Norris, M.D., and Horwitz, S.B. (1995): Altered expression of M beta 2, the class II beta-tubulin isotype, in a murine J774.2 cell line with a high level of taxol resistance. J Biol Chem. 270:31269–31275.

Hamill, D.R., Howell, B., Cassimeris, L., and Suprenant, K.A. (1998): Purification of a WD repeat protein, EMAP, that promotes microtubule dynamics through an inhibition of rescue. J. Biol. Chem. 273:9285–9291.

Hartman, J.J., Mahr, J., McNally, K., Okawa, K., Iwamatsu, A., Thomas, S., Cheesman, S., Heuser, J., Vale, R.D., and McNally, F.J. (1998). Katanin, a microtubule-severing protein, is a novel AAA ATPase that targets to the centrosome using a WD40-containing subunit. Cell 93:277–287.

Herzog, W., and Weber, K. (1978): Fractionation of brain microtubule-associated proteins. Eur. J. Biochem. 92:1–8.

Hiller, G., and Weber, K. (1978): Radioimmune assay for tubulin: A quantitative comparison of the tubulin content of different established tissue culture cells and tissues. Cell 14:795–804.

Hirokawa, N. (1994): Microtubule organization and dynamics dependent on microtubule-associated proteins. Curr. Opin. Cell Biol. 6:74–81.

Horwitz, S.B., Shen, H.-J., He, L., Dittmar, P., Neef, R., Chen, J., and Schubart, U.K. (1997): The microtubule-destabilizing activity of metablastin (p19) is controlled by phosphorylation. J. Biol. Chem. 272:8129–8132.

Hotani, H., and Hori, T. (1988): Dynamics of microtubules visualized by darkfield microscopy: Treadmilling and dynamic instability. Cell Motil Cytoskeleton 10:229–236.

Houliston, E., and Elinson, R.P. (1992): Microtubules and cytoplasmic reorganization in the frog egg. Curr. Top. Dev. Biol. 26:53–70.

Howell, B., Odde, D.J., and Cassimeris, L. (1997): Kinase and phosphatase inhibitors cause rapid alterations in microtubule dynamic instability in living cells. Cell Motil. Cytoskeleton 38:201–214.

Huyett, A., Kahana, J., Silver, P., Zeng, X., and Saunders, W.S. (1998): The Kar3p and Kip2p motors function antagonistically at the spindle poles to influence cytoplasmic microtubule numbers. J. Cell. Sci. 111:295–301.

Hyams, J.S., and Lloyd, C.W. (1994): In Hyams, J.S., and Lloyd, C.W. (eds.): ''Microtubules.'' New York: Wiley-Liss, 439 pp.

Hyman, A.A., and Karsenti, E. (1996): Morphogenetic properties of microtubules and mitotic spindle assembly. Cell 84:401–411.

Illenberger, S., Drewes, G., Trinczek, B., Biernat, J., Meyer, H.E., Olmsted, J.B., Mandelkow, E.-M., and Mandelkow, E. (1996): Phosphorylation of microtubule-associated proteins MAP2 and MAP4 by the protein kinase $p110^{mark}$. Phosphorylation sites and regulation of microtubule dynamics. J. Biol. Chem. 271:10834–10843.

Inoué, S., and Salmon, E.D. (1995): Force generation by microtubule assembly/disassembly in mitosis and related movements. Mol. Biol. Cell. 6:1619–1640.

Itoh, T.J., and Hotani, H. (1994): Microtubule-stabilizing activity of microtubule-associated proteins (MAPs) is due to increase in frequency of rescue in dynamic instability: Shortening length decreases with binding of MAPs onto microtubules. Cell Struct. Funct. 19:279–290.

Itoh, T.J., Hisanaga, S.-I., Hosoi, T., Kishimoto, T., and Hotani, H. (1997): Phosphorylation states of microtubule-associated protein 2 (MAP2) determine the regulatory role of MAP2 in microtubule dynamics. Biochemistry 36:12574–12582.

Jourdain, L., Curmi, P., Sobel, A., Pantaloni, D., and Carlier, M.-F. (1997): Stathmin: A tubulin-sequestering protein which forms a ternary T_2S complex with two tubulin molecules. Biochemistry 36:10817–10821.

Kirschner, M., and Mitchison, T. (1986): Beyond self-assembly: From microtubules to morphogenesis. Cell 45:329–342.

Larsson, N., Marklund, U., Melander, H.G., Brattsand, G., and Gullberg, M. (1997): Control of microtubule dynamics by oncoprotein 18: Dissection of the regulatory role of multisite phosphorylation during mitosis. Mol. Cell. Biol. 17:5530–5539.

Li, Q., and Joshi, H.C. (1995): gamma-tubulin is a minus end-specific microtubule binding protein. J. Cell. Biol. 131:207–214.

López, L.A., and Sheetz, M.P. (1995): A microtubule-associated protein (MAP2) kinase restores microtubule motility in embryonic brain. J. Biol. Chem. 270:12511–12517.

MacKintosh, C., and MacKintosh, R.W. (1994): Inhibitors of protein kinases and phosphatases. TIBS 19:444–448.

Mandelkow, E., and Mandelkow, E.M. (1995): Microtubules and microtubule-associated proteins. Curr. Opin. Cell. Biol. 7:72–81.

Marklund, U., Larsson, N., Gradin, H.M., Brattsand, G., and Gullberg, M. (1996): Oncoprotein 18 is a phosphorylation-responsive regulator of microtubule dynamics. EMBO J. 15:5290–5298.

Masson, D., and Kreis, T.E. (1995): Binding of E-MAP-115 to microtubules is regulated by cell cycle-dependent phosphorylation. J. Cell. Biol. 131:1015–1024.

McIntosh, J.R. (1984): Microtubule catastrophe. Nature 312:196–197.

Mitchison, T., and Kirschner, M.W. (1984a): Microtubule assembly nucleated by isolated centrosomes. Nature 312:232–237.

Mitchison, T.J., and Kirschner, M.W. (1984b): Dynamic instability of microtubule growth. Nature 312:237–242.

Moore, R.C., Zhang, M., Cassimeris, L., and Cyr, R.J. (1997): In vitro assembled plant microtubules exhibit a high state of dynamic instability. Cell Motil. Cytoskeleton 38:278–286.

Murray, A. (1991): Cell cycle extracts. In Kay, B.K., and Peng, H.B. (eds): ''*Xenopus laevis:* Practical Uses in Cell and Molecular Biology.'' San Diego: Academic Press, pp. 581–605.

Oliver, J.M. (1978): Cell biology of leukocyte abnormalities—membrane and cytoskeletal function in normal and defective cells. Am. J. Pathol. 93:221–259.

Olmsted, J.B. (1986): Microtubule associated proteins. Ann. Rev. Cell. Biol. 2:421–457.

Olmsted, J.B., Stemple, D.L., Saxton, W.M., Neighbors, B.W., and McIntosh, J.R. (1989): Cell cycle-dependent changes in the dynamics of MAP 2 and MAP 4 in cultured cells. J. Cell. Biol. 109:211–223.

Ookata, K., Hisanaga, S., Bulinski, J.C., Murofushi, H., Aizawa, H., Itoh, T.J., Hotani, H., Okumura, E., Tachibana, K., and Kishimoto, T. (1995): Cyclin B interaction with microtubule-associated protein 4 (MAP4) targets p34cdc2 kinase to microtubules and is a potential regulator of M-phase microtubule dynamics. J. Cell Biol. 128:849–862.

Ookata, K., Hisanaga, S.-T., Sugita, M., Okuyama, A., Murofushi, H., Kitazawa, H., Chari, S., Bulinski, J.C., and Kishimoto, T. (1997): MAP4 is the in vivo substrate for cdc2 kinase in HeLa cells: Identification of an M-phase specific and a cell cycle-independent phosphorylation site in MAP4. Biochemistry 36: 15873–15883.

Panda, D., Miller, H.P., Banerjee, A., Luduena, R.F., and Wilson, L. (1994): Microtubule dynamics in vitro are regulated by the tubulin isotype composition. Proc. Natl. Acad. Sci. U.S.A. 91:11358–11362.

Parsons, S.F., and Salmon, E.D. (1997): Microtubule assembly in clarified *Xenopus* egg extracts. Cell Motil. Cytoskeleton 36:1–11.

Pryer, N.K., Walker, R.A., Skeen, V.P., Bourns, B.D., Soboeiro, M.F., and Salmon, E.D. (1992): Brain microtubule-associated proteins modulate microtubule dynamic instability in vitro. Real-time observations using video microscopy. J. Cell Sci. 103:965–976.

Sammak, P.J., and Borisy, G.G. (1988): Direct observation of microtubule dynamics in living cells. Nature 332:724–726.

Schulze, E., and Kirschner, M. (1988): New features of microtubule behaviour. Nature 334:356–359.

Scott, C.W., Spreen, R.C., Herman, J.L., Chow, F.P., Davison, M.D., Young, J., and Caputo, C.B. (1993): Phosphorylation of recombinant tau by cAMP-dependent protein kinase. Identification of phosphorylation sites and effect on microtubule assembly. J. Biol. Chem. 268:1166–1173.

Shamu, C.E., and Murray, A.W. (1992): Sister chromatid separation in frog egg extracts requires DNA topoisomerase II activity during anaphase. J Cell Biol 117:921–934.

Shelden, E., and Wadsworth, P. (1993): Observation and quantification of individual microtubule behaviour in vivo: Microtubule dynamics are cell-type specific. J. Cell Biol. 120:935–945.

Shiina, N., Gotoh, Y., and Nishida, E. (1992): A novel homo-oligomeric protein responsible for an MPF-dependent microtubule severing activity. EMBO J. 11:4723–4731.

Shiina, N., Moriguchi, T., Ohta, K., Gotoh, Y., and Nishida, E. (1992): Regulation of a major microtubule-associated protein by MPF and MAP kinase. EMBO J. 11:3977–3984.

Simon, J.R., Parsons, S.F., and Salmon, E.D. (1992): Buffer conditions and non-tubulin factors critically affect the microtubule dynamic instability of sea urchin egg tubulin. Cell Motil. Cytoskeleton 21:1–14.

Sobel, A. (1991): Stathmin: a relay phosphoprotein for multiple signal transduction? Trends Biochem. Sci. 16:301–305.

Tanaka, E.M., and Kirschner, M.W. (1991): Microtubule behavior in the growth cones of living neurons during axon elongation. J. Cell Biol. 115:345–363.

Tournebize, R., Andersen, S.S.L., Verde, F., Dorée, M., Karsenti, E., and Hyman, A.A. (1997): Distinct roles of PP1 and PP2A-like phosphatases in control of microtubule dynamics during mitosis. EMBO J. 16:5537–5549.

Vale, R.D. (1991): Severing of stable microtubules by a mitotically activated protein in *Xenopus* egg extracts. Cell 64:827–839.

Vallee, R.B. (1982): A taxol-dependent procedure for the isolation of microtubules and microtubule-associated proteins (MAPs). J. Cell Biol. 92:435–442.

Vasquez, R.J., Gard, D.L., and Cassimeris, L. (1994): XMAP from *Xenopus* eggs promotes rapid plus end assembly of microtubules and rapid microtubule polymer turnover. J. Cell Biol. 127:985–993.

Verde, F., Labbé, J.C., Dorée, M., and Karsenti, E. (1990): Regulation of microtubule dynamics by cdc2 protein kinase in cell-free extracts of *Xenopus* eggs. Nature 343:233–238.

Verde, F., Dogterom, M., Stelzer, E., Karsenti, E., and Leibler, S. (1992): Control of microtubule dynamics and length by cyclin A and cyclin B dependent kinases in *Xenopus* egg extracts. J. Cell Biol. 118:1097–1108.

Vorobjev, I.A., Svitkina, T.M., and Borisy, G.G. (1997): Cytoplasmic assembly of microtubules in cultured cells. J. Cell Sci. 110:2635–2645.

Voter, W.A., and Erickson, H.P. (1984): The kinetics of microtubule assembly. J. Biol. Chem. 259:10430–10438.

Walczak, C.E., Mitchison, T.J., and Desai, A. (1996): XKCM1: A *Xenopus* kinesin-related protein that regulates microtubule dynamics during mitotic spindle assembly. Cell 84:37–47.

Walczak, C.E., Vernos, I., Mitchison, T.J., Karsenti, E., and Heald, R. (1998): A model for the proposed roles of different microtubule-based motor proteins in establishing spindle bipolarity. Curr. Biol. 8:903–913.

Walker, R.A., O'Brien, E.T., Pryer, N.K., Sobeiro, M.F., Voter, W.A., Erickson, H.P., and Salmon, E.D. (1988): Dynamic instability of individual microtubules analyzed by video light microscopy: Rate constants and transition frequencies. J. Cell Biol. 107:1437–1448.

Waterman-Storer, C.M., and Salmon, E.D. (1997): Microtubule dynamics: treadmilling comes around again. Curr. Biol. 7:R369–R372.

Waters, J.C., and Salmon, E.D. (1997): Pathways of spindle assembly. Curr. Opin. Cell Biol. 9:37–43.

Weisenberg, R.C. (1972): Microtubule formation in vitro in solutions containing low calcium concentrations. Science 177:1104–1105.

Wiche, G., Oberkanins, C., and Himmler, A. (1991): Molecular structure and function of microtubule-associated proteins. Int. Rev. Cytol. 124:217–273.

Zhai, Y., Kronebusch, P.J., Simon, P.M., and Borisy, G.G. (1996): Microtubule dynamics at the G2/M transition: Abrupt breakdown of cytoplasmic microtubules at nuclear envelope breakdown and implications for spindle morphogenesis. J. Cell Biol. 135:201–214.